(11) Tatsuma, T.; Watanabe, T. *Anal. Chem.* **1991**, *63*, 1580-1585.
(12) Foulds, N. C.; Lowe, C. R. *J. Chem. Soc., Faraday Trans. 1* **1986**, *82*, 1259-1264.
(13) Umana, M.; Waller, J. *Anal. Chem.* **1986**, *58*, 2979-2983.
(14) Foulds, N. C.; Lowe, C. R. *Anal. Chem.* **1988**, *60*, 2473-2478.
(15) Iwakura, C.; Kajiya, Y.; Yoneyama, H. *J. Chem. Soc., Chem. Commun.* **1988**, 1019-1020.
(16) Yabuki, S.; Shinohara, H.; Aizawa, M. *J. Chem. Soc., Chem. Commun.* **1989**, 945-946.
(17) Bartlett, P. N.; Whitaker, R. G. *J. Electroanal. Chem. Interfacial Electrochem.* **1987**, *224*, 37-48.
(18) Belanger, D.; Nadreau, J.; Fortier, G. *J. Electroanal. Chem. Interfacial Electrochem.* **1989**, *274*, 143-155.
(19) Diaz, A. F.; Crowley, J.; Bargon, J.; Gardini, G. P.; Torrance, J. B. *J. Electroanal. Chem. Interfacial Electrochem.* **1981**, *121*, 355-361.
(20) Waltman, R. J.; Bargon, J. *Tetrahedron* **1984**, *40*, 3963-3970.
(21) Hayashi, Y.; Yamazaki, I. *J. Biol. Chem.* **1979**, *254*, 9101-9106.
(22) Diaz, A. F.; Castillo, J. I.; Logan, J. A.; Lee, W. Y. *J. Electroanal. Chem. Interfacial Electrochem.* **1981**, *129*, 115-132.
(23) Kajiya, Y.; Tsuda, R.; Yoneyama, H. *J. Electroanal. Chem. Interfacial Electrochem.* **1991**, *301*, 155-164.

RECEIVED for review December 2, 1991. Accepted February 18, 1992.

Dynamics of Organic Compound Extraction from Water Using Liquid-Coated Fused Silica Fibers

Derek Louch, Safa Motlagh, and Janusz Pawliszyn*

Guelph-Waterloo Center for Graduate Work in Chemistry and the Waterloo Center for Groundwater Research, University of Waterloo, Waterloo, Ontario, Canada N2L 3G1

Solid-phase microextraction (SPME) is an inexpensive, rapid, and solvent-free extraction method for the isolation of organic compounds from an aqueous sample. The technique uses a few centimeters of poly(dimethylsiloxane)-coated fused silica optical fiber which is mounted for convenience and ruggedness into a microsyringe. The organic contaminants are extracted into the coating and transferred for thermal desorption and analysis into the injector of a gas chromatograph. Mathematical descriptions of the absorption and desorption processes were developed and compared with experimental results. One model assumes a perfectly agitated solution which results in extraction times dependent only on diffusion of analyte in the coating. The second model considers extraction from a static solution. In this case extraction times are determined by diffusion of analyte in water. These models facilitate a better understanding of the extraction process. Results indicate that when standard stirring equipment is used as a means of agitation, the dynamics of the extraction process is controlled by diffusion of analyte through the thin static aqueous layer located around the fiber. Extraction times for benzene, toluene, and *p*-xylene using a coating thickness of 55 μm are under 10 min and can be shortened substantially when more efficient agitation methods are used. The technique allows sub-ppb determination of organics in water with flame ionization detection. The linear range of the method is over several orders of magnitude. The sensitivity of the technique is dependent on the coating volume and the coating/water distribution constant. The relative precision of the method is a few percent and is dependent on the thickness of the coating. Using this technique, poly(dimethylsiloxane)/water distribution constants were determined for benzene (125), toluene (294), and *p*-xylene (831) and are similar to corresponding values for octanol/water distribution constants.

INTRODUCTION

The contamination of water supplies by organic pollutants has become a major concern to the public which demands better control and monitoring of this important resource. To achieve this goal, frequent analysis of water samples is required. In the first step of the analytical process the organic contaminants are separated from the aqueous matrix. The separation techniques are divided into two major groups:[1] concentration methods, in which water is removed and the dissolved substances are left behind, and isolation methods in which the dissolved substances are removed from water. Isolation techniques are the more commonly used methods in the analysis of organics in water. Volatiles are usually analyzed by the use of purge and trap which is a U.S. Environmental Protection Agency (EPA) approved technique,[2] stripping and headspace analysis. These methods either require expensive instrumentation or are not sufficiently sensitive. Nonvolatiles are analyzed primarily by the use of liquid-liquid extraction (LLE), which is an EPA approved technique,[2] and solid-phase extraction (SPE). These methods are generally time consuming, are difficult to automate, and use expensive high purity toxic organic solvents.

Recently a novel technique, solid-phase microextraction (SPME), was proposed which solves many of the problems associated with the more traditional methods.[3,4] In this procedure, a small diameter optical fiber coated with a polymeric phase is placed in an aqueous sample. The analytes partition into the stationary phase and are then thermally desorbed, on-column, in the injector of a gas chromatograph. Since the coatings used are almost always viscous liquids, the extraction is, in effect, a nonexhaustive liquid-liquid extraction with the convenience that the "organic phase" is attached to the fiber. This fiber is contained in a syringe which protects it and simplifies introduction of the fiber into a gas chromatographic (GC) injector. The total analysis time is only a few minutes.[3] Optical fibers are used because they are inexpensive and are made of chemically inert fused silica, the same material used to make capillary GC columns. They have a small diameter which allows convenient introduction into a chromatographic injector. These fibers coated with polymers such as poly(dimethylsiloxane) of various thicknesses are available commercially and can be used directly in extractions. The uncoated fiber[3] can also be used or a variety of common chromatographic stationary phases can be attached to its surface.[4] This technique can be applied successfully to the analysis of volatile chlorinated organics such as chlorinated organic solvents and substituted benzenes as well as nonvo-

0003-2700/92/0364-1187$03.00/0

latile chlorinated biphenyls. SPME avoids several disadvantages associated with more established techniques such as the emulsion problems and high solvent consumption of LLE, memory effects of purge and trap and the high blank values sometimes associated with SPE. Using this extremely simple and fast technique, one can sample in the field or on-line and can analyze small (<1 mL) sample volumes. The simple geometry of the fiber ensures that the extraction can be performed directly on real samples without concerns of plugging (unlike SPE).

Since in SPME an exhaustive extraction does not occur, but an equilibrium is developed between the aqueous and "stationary" organic phase, the number of moles of analyte absorbed by the fiber, n_1, is linearly related to the concentration of analyte in the aqueous phase by the equation

$$n_1 = \kappa V_1 C_2^0 = A C_2^0 \quad (1)$$

where V_1 is the volume of the coating, C_2^0 is the concentration in the aqueous phase, κ is the distribution constant, and $A = \kappa V_1$. This equation considers only the mass absorbed at equilibrium and cannot take into account the finite time needed for the coating to absorb the analyte. In this paper a dynamic model was developed which mathematically describes the extraction process. It facilitates an understanding of the relationship between geometric and thermodynamic parameters on the efficiency and speed of the extraction.

THEORY

During the solid-phase microextraction (SPME) procedure, a length of polymer-coated fused silica fiber is immersed into an aqueous solution of analyte contained in a vial (Figure 1) where the analyte partitions between the polymer and the water. The extraction is completed when the system reaches equilibrium. The fiber containing the absorbed analytes is then removed from solution and transferred to the injector of a gas chromatograph (GC) for desorption and analysis.

As shown in Figure 1, the system has cylindrical geometry; a, b, and d are the radii of the silica rod, the coated fiber, and the vial, respectively, L is the length of the coated portion of the fiber, κ is the coating/water distribution constant of the analyte, D_1 and D_2 are the diffusion coefficients of the analyte in the coating and water, respectively, and C_1 and C_2 describe the concentration distribution of analyte in the organic coating and the aqueous solution respectively.

The discussion below assumes that the dynamics of extraction is a diffusion limited process. Thus, diffusion is the only mass transport mechanism which determines the migration of the analyte molecules in the system. This assumption is valid only if the polymer coating is a normal liquid and, as a consequence, there is no activation energy involved in the transfer of analyte between solution and coating. If the polymer is a solid (i.e. below its crystallization temperature), this assumption may not be accurate. The model also assumes that, as the concentration of analyte in solution is increased, the physical properties of the polymer do not change, i.e. the polymer neither swells nor does the diffusion coefficient of the analyte in the polymer depend on analyte concentration. If the polymer were glassy (i.e. below its glass transition temperature), this would not be an accurate assumption. The model does not account for the mass of analyte absorbed through the surface at the bottom of the coated fiber. This is a valid assumption when the length of the coated portion of the fiber is much larger than its diameter since in this situation the surface area at the bottom of the fiber is a very small portion of the total surface area. In practical experiments this ratio exceeds 100:1.

The above assumptions allow a mathematical description of the extraction dynamics of the system by solving the differential equation which is often referred to as Fick's second law of diffusion:[5]

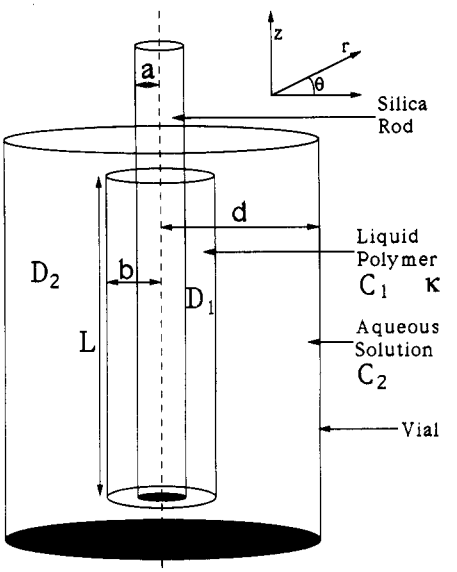

Figure 1. Graphic representation of the coated fiber inserted into a finite volume of unstirred solution where κ is the coating/water distribution constant of the analyte, D_1 is the diffusion coefficient of the analyte in the coating, D_2 is the diffusion coefficient of the analyte in the water, C_1 is the concentration of analyte in the coating, C_2 is the concentration of analyte in the water, L is the height of the cylinder exposed to solution, a is the radius of the silica fiber, b is the radius of the coated fiber, and d is the radius of the analyte container.

$$D\left(\frac{\partial^2 C}{\partial x^2} + \frac{\partial^2 C}{\partial y^2} + \frac{\partial^2 C}{\partial z^2}\right) = \frac{\partial C}{\partial t} \quad (2)$$

where D is the diffusion coefficient of the analyte and C is its concentration. This equation can be converted from rectangular to cylindrical coordinates which is easier to solve because of the cylindrical symmetry of our system:[5]

$$D\left[\frac{1}{r}\frac{\partial}{\partial r}\left(r\frac{\partial C}{\partial r}\right) + \frac{1}{r^2}\frac{\partial^2 C}{\partial \theta^2} + \frac{\partial^2 C}{\partial z^2}\right] = \frac{\partial C}{\partial t} \quad (3)$$

Considering the cylindrical geometry of our fiber and the diffusion process, we see that the concentration profile in the polymer does not vary along the axis of the fiber (i.e. on z) nor does it depend on the radial angle from the center of the fiber (i.e. on θ) (see Figure 1). Therefore the terms containing derivatives along these coordinates will vanish.

$$\frac{\partial^2 C}{\partial r^2} + \frac{1}{r}\frac{\partial C}{\partial r} = \frac{1}{D}\frac{\partial C}{\partial t} \quad (4)$$

The solution to the above differential equation with the appropriate boundary conditions corresponding to our experimental configuration will describe the concentration profile of the analyte in the system as a function of radius. Then the total mass absorbed by the coating as a function of time can be calculated by integrating the concentration profile along the radius:

$$M = 2\pi L \int_a^b C_1(r,t) r \, dr \quad (5)$$

where L is the height of the cylinder, a is the radius of the silica rod, and b is the radius of the coated fiber (Figure 1). The resulting relationship can be easily verified experimentally by determining the mass of analyte absorbed by the fiber after the fiber has been extracting for a specific time.

Two models have been derived, and each of them describes a limiting case. In the first model we assume a perfectly

agitated analyte solution. In this situation, the migration of the analyte into the organic coating is not affected by diffusion in the aqueous phase. The second model assumes an unstirred solution where the analyte must penetrate a water layer surrounding the fiber before it can diffuse into the coating. Neither of these models describes attainable experimental conditions, since it is neither possible to ensure perfect agitation of the solution nor possible to eliminate mixing through convection. However, an understanding of the relationship between the different geometric and physical parameters and the extraction dynamics of these two limiting cases will allow us to interpret experimental data and to optimize extraction conditions.

Diffusion of Analyte into the Fiber Coating from a Perfectly Agitated Solution of Infinite Volume. This model describes the fastest possible extraction of analytes from water since the diffusion in water is neglected. This situation relates to the absorption process from a large volume of well-stirred solution in a laboratory or from rapidly moving waters such as streams or rivers. The boundary conditions required to solve eq 3 are determined on the basis of the aforementioned assumptions. The concentration of the analyte in the stationary phase at the start of the experiment is known:

$$C_1(r,t=0) = C_1^0 \tag{6}$$

When considering an extraction $C_1^0 = 0$, but for a desorption, $C_1^0 > 0$. The exterior surface of the coated fiber is maintained at a constant analyte concentration which is determined by the concentration of analyte in the aqueous phase adjacent to the fiber and by the distribution constant of the analyte between the coating and the solution:

$$C_1(r=b,t) = \kappa C_2(r=b,t) \tag{7}$$

The assumption of infinite volume of perfectly agitated solution ensures that $C_2(r = b, t)$ is constant and it is equal to the concentration of analyte in solution before the extraction, C_2^0. The fused silica rod is considered to be impenetrable to analyte molecules:

$$\frac{\partial C_1}{\partial r}(r=a,t) = 0 \tag{8}$$

The analytical solution to eq 3 with the above initial and boundary conditions (eqs 6–8) can be obtained by using the method of Separation of Variables (see Appendix). The concentration profile in the coating as a function of time is described by

$$C_1(r,t) = \kappa C_2^0 + (C_1^0 - \kappa C_2^0)\pi \sum_{m=0}^{\infty} \exp(-\alpha_m^2 D_1 t)\frac{J_1(\alpha_m b)J_1(\alpha_m a)}{J_0^2(\alpha_m b) - J_1^2(\alpha_m a)}[Y_0(\alpha_m r)J_1(\alpha_m a) - Y_0(\alpha_m a)J_0(\alpha_m r)] \tag{9}$$

where the α_m's are the roots of

$$J_0(\alpha b)Y_1(\alpha a) - J_1(\alpha a)Y_1(\alpha b)$$

and J, Y are Bessel functions.

Although the solution is analytical, the values obtained from this equation are still only approximations since they require an infinite summation. However the series converges and therefore a good estimate of the true value can be obtained by summing a finite number of terms (ten or more). Figure 2 illustrates the general relationships described mathematically by eq 9. The graph is presented in dimensionless coordinates and considers all possible fiber geometries, analyte properties and concentrations. The vertical axis corresponds to the fraction of equilibrium concentration $C/\kappa C_2^0$ and the horizontal axis corresponds to the relative depth in the coating

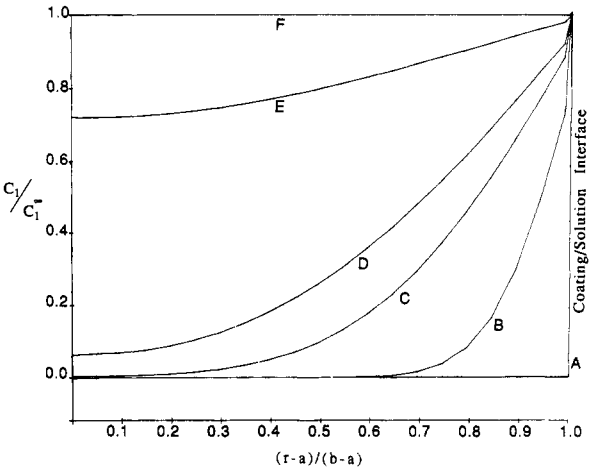

Figure 2. Absorption concentration profile in a fiber coating, with initial analyte in fiber concentration equal to zero: curve A, $D_1t/(b-a)^2 = 0$; curve B, $D_1t/(b-a)^2 = 0.01$; curve C, $D_1t/(b-a)^2 = 0.05$; curve D, $D_1t/(b-a)^2 = 0.1$; curve E, $D_1t/(b-a)^2 = 0.5$; curve F, $D_1t/(b-a)^2 = \infty$.

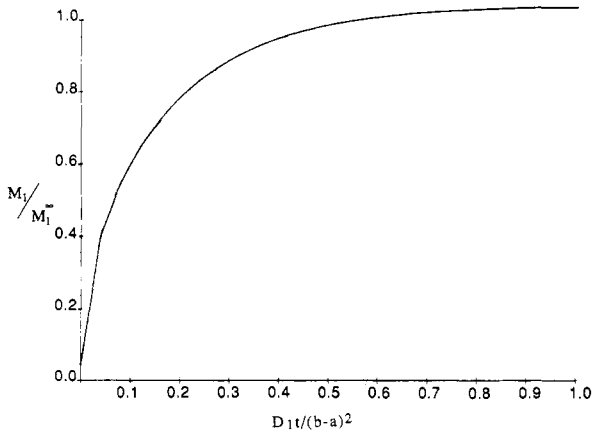

Figure 3. Mass absorbed from a perfectly agitated solution of infinite volume with the same parameters as in Figure 2.

$(r-a)/(b-a)$. It is possible to describe any specific case using this general graph. The series of curves in Figure 2 correspond to different immersion times of the fiber into the aqueous solution. Here, time is represented by the unit-free $D_1t/(b-a)^2$. The family of curves in Figure 2 represent concentration profiles of analyte in the coating at different stages of the extraction. The concentration of analyte in the aqueous phase is uniform and constant (i.e. does not change with time) and is therefore equal to the initial concentration C_2^0. This is ensured by the infinite volume and perfect agitation conditions.

Before the fiber is placed in the solution, no analyte is present in the coating (Figure 2A). Immediately after immersion into solution, only a thin layer close to the surface contains analyte (Figure 2B). With time, analyte molecules diffuse progressively deeper into the coating (Figures 2C–E) and eventually reach equilibrium (Figure 2F). The slope of the concentration distribution in the coating (which corresponds to the concentration gradient) decreases rapidly with time. The gradient determines the flux of the analyte into the coating as given by the Fick's first law:

$$F = -D_1 \frac{dC}{dr} \tag{10}$$

where F is flux of analyte molecules (mol s^{-1} m^{-2}). Diffusion stops after the gradient drops to zero at equilibrium. However, this is only a hypothetical situation since in reality, equilibrium

is reached after an infinitely long time.

The area under the concentration profile curves from Figure 2 corresponds to the amount of analyte in the coating expressed as a fraction of the (maximum) mass extracted at equilibrium (Figure 2F). Approximately 50% of the maximum amount is extracted after 0.1 time units (Figure 2D) while it takes about 5 times longer to extract about 90% of the maximum amount (Figure 2E). This relationship can be described mathematically by integrating the concentration distribution function (eq 9) over the radius and thus obtaining the mass absorbed by the coating as a function of time:

$$M_1 = 2\pi L\left\{\kappa C_2^0\left[\frac{r^2}{2}\right]_a^b + (C_1^0 - \kappa C_2^0)\pi\sum_{m=1}^{\infty}\exp(-\alpha^2 D_1 t)\left[\gamma\left[\frac{rJ_1(\alpha_m r)}{\alpha_m}\right]_a^b - \delta\left[\frac{rY_1(\alpha_m r)}{\alpha_m}\right]_a^b\right]\right\} \quad (11)$$

where

$$\gamma = \frac{J_1^2(\alpha_m a)Y_0(\alpha_m b)}{J_1^2(\alpha_m a) - J_0^2(\alpha_m b)}$$

and

$$\delta = \frac{J_1^2(\alpha_m a)J_0(\alpha_m b)}{J_1^2(\alpha_m a) - J_0^2(\alpha_m b)}$$

The relationship described by eq 11 is shown in Figure 3 and is referred to as the time exposure profile of the fiber. This single graph considers all possible cases. The vertical axis values correspond to the relative mass absorbed by the coating compared to the equilibrium value M_1^∞. The horizontal axis is in the dimension-free unit $D_1t/(b-a)^2$ corresponding to the family of curves from Figure 2. Here again, there is an initial dramatic increase in the mass absorbed by the fiber which then evens out and eventually reaches equilibrium. About 90% of M_1^∞ is absorbed after time corresponding to $D_1t/(b-a)^2 = 0.5$. In this paper this time is referred to as the equilibration time. For practical situations the equilibration time for a perfectly agitated solution can be calculated from this relationship by substituting specific diffusion coefficients and fiber thicknesses. For example, the expected equilibration time for the determination of benzene in water is about 20 s when using 100-μm-thick poly(dimethylsiloxane) coating in which the diffusion coefficient of this analyte is about 2.8×10^{-6} cm^2/s.[6]

Interesting information about the extraction process can be obtained by analyzing Figures 2 and 3. Equilibration time is inversely proportional to diffusion coefficient. Therefore, it is expected that the extraction time will be much longer for more cross-linked or more viscous polymers. The application of such materials might be necessary in order to improve the thermal stability of the coatings which can be used in the analysis of nonvolatile compounds. High molecular weight compounds are expected to have longer equilibration times than low molecular weight analytes because of their smaller diffusion coefficients.

Equation 9 and Figure 2 clearly illustrate that, under perfect agitation conditions, the speed of the absorption process is determined only by the diffusion of analyte in the polymer coating. Equilibration time is proportional to the square of the coating thickness. Therefore, if it is necessary to improve the sensitivity of the technique by increasing the phase ratio, and as a consequence the coating thickness, a significant increase in the extraction time will occur. However this increase in phase ratio can also be accomplished without affecting the equilibration time by using the same coating thickness on a thicker silica rod. Using a thicker rod results in an increase in the total volume of the "stationary phase"

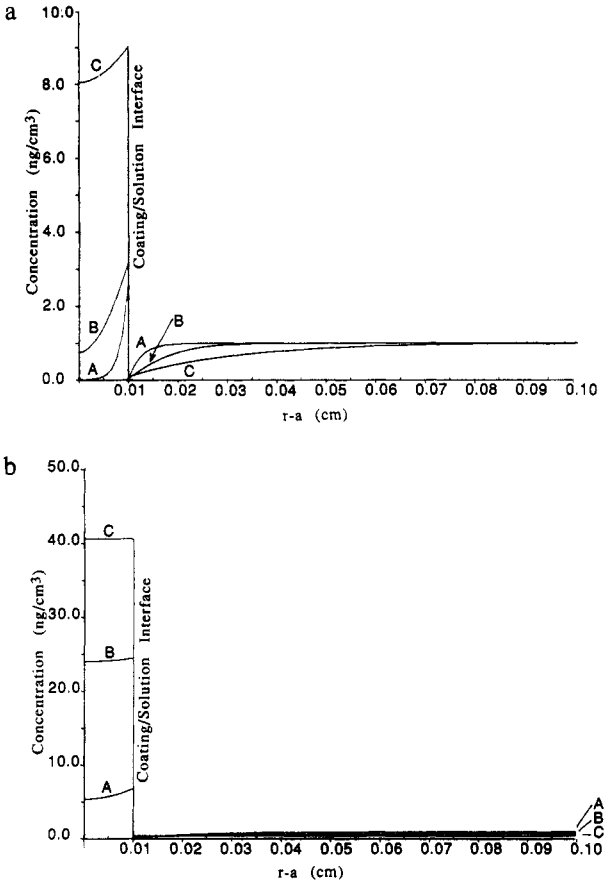

Figure 4. (a) Concentration profile in a coated fiber, with $\kappa = 100$, $C_1 = 0$, $C_2 = 1 \times 10^{-6}$ g/cm^3, $D_2 = 1.08 \times 10^{-5}$ cm^2/s, $D_1 = 2.8 \times 10^{-6}$ cm^2/s, $a = 0.005$ cm, $b = 0.015$ cm and $d = 0.1$ cm. Curves: A = 0.6 s, B = 6 s, C = 60 s after immersion of fiber into solution. (b) Curves: A = 36 s, B = 360 s, C = 3600 s after immersion of fiber into solution.

but keeps the coating thickness and the surface to volume ratio constant. Similar results can be obtained by increasing the length of the fiber exposed to the solution.

According to eq 1, the amount of analyte absorbed and consequently the sensitivity of the method is also proportional to the distribution constant. This parameter does not effect the speed of the extraction when considering the perfectly stirred solution. With an increase in κ, a higher flux of analyte into the coating is necessary to keep the equilibration time the same; this is achieved by the formation of higher concentration gradients at the coating/solution interface (Figure 2).

The situation discussed above describes an ideal situation where the effect of diffusion in water is neglected by assuming perfect stirring of the aqueous solution during the extraction process. In reality, there is always a thin layer of unstirred water around the fiber. A higher stirring rate will result in a thinner layer. To understand how the dynamics of extraction are affected by diffusion though water we consider extraction from an unagitated solution.

Diffusion of Analyte into the Fiber Coating from an Unagitated Solution of Finite Volume. The situation discussed in this model corresponds to sampling from an unstirred solution in a laboratory or from stagnant waters such as ponds or ditches. This model can take into account the depletion of analyte from solution since in this case the volume of solution is limited.

As in the well-agitated case, the mathematical description of the process can be obtained by solving eq 4 and assuming appropriate boundary conditions. The first initial condition

requires that no analyte be present in the coating at the start of the experiment:

$$C_1(r,t=0) = 0 \tag{12}$$

but that all of the analyte be present in the aqueous solution:

$$C_2(r,t=0) = C_2^0 \tag{13}$$

As in the previous case, it is assumed that the concentration of analyte at the inner surface of the coating is always κ times the concentration of analyte in solution at the outer surface of the coating (eq 7). Because of mass balance, the fluxes of analyte at the inner and the outer surfaces of the coating must be equal:

$$D_1 \frac{\partial C_1}{\partial r}(r=b,t) = D_2 \frac{\partial C_2}{\partial r}(r=b,t) \tag{14}$$

In addition to the requirement that the interior of the fiber be impenetrable (eq 8), a similar requirement is put on the interior surface of the vial:

$$\frac{\partial C_2}{\partial r}(r=d,t) = 0 \tag{15}$$

It is very difficult to obtain an analytical solution for this case since two different phases are involved. Therefore, the method of finite differences was used to obtain a numerical solution to the above equations. The following system of linear equations must be solved in order to obtain the concentrations at different time intervals:

At $i = 1$ ($r = a$),
i.e. at the fused silica-coating interface

$$-\left[\frac{2D_1}{(\Delta r)^2} + \frac{1}{\Delta t}\right] C_{1\,1}{}^n + \frac{2D_1}{(\Delta r)^2} C_{1\,2}{}^n = -\frac{1}{\Delta t} C_{1\,1}{}^{n-1} \tag{16}$$

At $i = 1, 2, 3, ..., M - 1$ ($a < r < b$), i.e. in the coating,

$$\left[\frac{2D_1 i - D_1}{2i(\Delta r)^2}\right] C_{1\,i-1}{}^n - \left[\frac{2D_1}{(\Delta r)^2} + \frac{1}{\Delta t}\right] C_{1\,i}{}^n + \left[\frac{2D_1 i + D_1}{2i(\Delta r)^2}\right] C_{1\,i+1}{}^n = -\frac{1}{\Delta t} C_{1\,i}{}^{n-1} \tag{17}$$

At $i = M$ ($r = b$), i.e. at the coating–solution interface,

$$-\frac{D_1}{\Delta r} C_{1\,M-1}{}^n + \frac{D_1}{\Delta r} C_{1\,M}{}^n + \frac{D_2}{\Delta r} C_{2\,M}{}^n - \frac{D_2}{\Delta r} C_{2\,M+1}{}^n = 0 \tag{18}$$

and

$$C_{1\,M}{}^n - \kappa C_{2\,M}{}^n = 0 \tag{19}$$

At $i = M + 1, M + 2, ..., N - 1$ ($b < r < d$),
i.e. in the solution

$$\left[\frac{2D_2 i - D_2}{2i(\Delta r)^2}\right] C_{2\,i-1}{}^n - \left[\frac{2D_2}{(\Delta r)^2} + \frac{1}{\Delta t}\right] C_{2\,i}{}^n + \left[\frac{2D_2 i + D_2}{2i(\Delta r)^2}\right] C_{2\,i+1}{}^n = -\frac{1}{\Delta t} C_{2\,i}{}^{n-1} \tag{20}$$

At $i = N$ ($r = d$),
i.e. at the solution–container interface

$$\frac{2D_2}{(\Delta r)^2} C_{2\,N-1}{}^n - \left[\frac{2D_2}{(\Delta r)^2} + \frac{1}{\Delta t}\right] C_{2\,N}{}^n = -\frac{1}{\Delta t} C_{2\,N}{}^{n-1} \tag{21}$$

The solution to the above equations can be represented as a family of graphs which describe the progress of the extraction process for a specific case. Figure 4 shows a family of curves, each of which describes the concentration profile in the fiber and the solution at a different time during the extraction of benzene from water. Diffusion into a 100-μm-thick poly(dimethylsiloxane) coating covering a 100-μm-o.d. fiber rod inserted into a 2-mm-i.d. vial containing 1 ppb of aqueous sample was modeled. Unless otherwise indicated, the literature values for the diffusion coefficients of benzene in poly(dimethylsiloxane), i.e. 2.8×10^{-6} cm^2/s,[6] and in water, i.e. 1.08×10^{-5} cm^2/s[7] were used in the calculations. Figure 4a shows the early stages of the extraction process. As in the well agitated case (Figure 2), at the initial stages of the extraction, the analyte is present in the thin layer of the polymer which is close to the aqueous solution (Figure 4a-A). However, the analyte concentration is much lower compared with the stirred case since the layer of solution close to the fiber is now depleted of analyte and a concentration profile has now also formed in the aqueous phase. Transport of the analyte through the progressively thicker depleted layer determines the extraction speed (Figure 4a-A–C). Figure 4b illustrates the concentration distribution of analyte in the system at more advanced stages of the extraction. It takes about 400 s (Figure 4b-B) for the system to extract almost half of the equilibrium amount (Figure 4b-C). This is over 2 orders of magnitude longer compared to the well-agitated case (Figure 2D). It should also be noted that in this case, after the extraction was complete, the concentration of analyte in the aqueous phase dropped to about 20% of its original value. This is a result of the high distribution constant and the small volume of the aqueous sample. This example demonstrates that it is possible to obtain an exhaustive extraction when, at equilibrium, most of the analyte is in the stationary phase. In this situation, eq 1 no longer applies since the concentration of analyte in the aqueous solution changes substantially during the extraction. To derive the analogous equation to eq 1 which can take into account the depletion of the analyte in the aqueous phase we consider a mass balance equation which relates analyte concentrations before and after the extraction:

$$n_1 + C_2{}^\infty V_2 = C_2{}^0 V_2 \tag{22}$$

where $C_2{}^\infty$ is the concentration of benzene in the aqueous phase at equilibrium, $C_2{}^0$ is the initial concentration of benzene in the aqueous phase, and V_2 is the volume of the aqueous sample. Substituting

$$\kappa = \frac{C_1{}^\infty}{C_2{}^\infty} \tag{23}$$

into the above equation and simplifying, the following relationship is obtained:

$$n_1 = \frac{\kappa V_1 V_2 C_2{}^0}{\kappa V_1 + V_2} \tag{24}$$

It should be noted that the amount of analyte absorbed by the coating is proportional to the initial analyte concentration for both the infinite volume case and the finite volume case. However the additional term κV_1 is now present in the denominator of the more general equation. The presence of this new term in the equation decreases the amount of analyte absorbed by the coating, but this decrease is significant only when this term is comparable to the volume of the aqueous phase V_2. In practice this occurs only for a large κ since the volume of stationary phase in SPME is very small. For very large distribution constants, $\kappa V_1 \gg V_2$ and therefore most of the analyte is in the coating. In this case, the extraction is, for all practical purposes, quantitative. To ensure that more

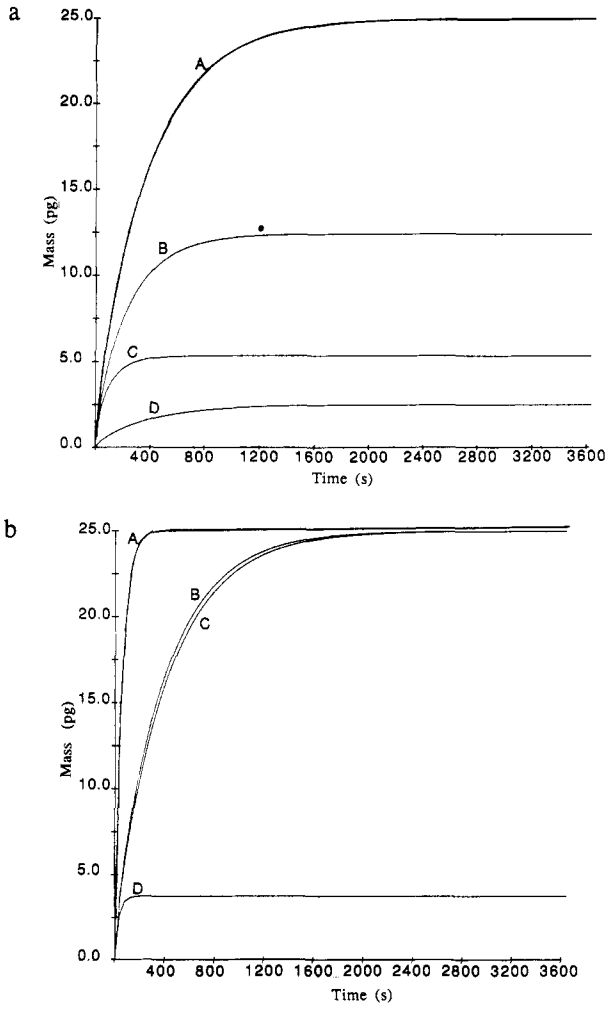

Figure 5. (a) Mass absorbed by the 1-cm-long fiber in Figure 4 with the same parameters except for the following: curve A, $b - a = 100$ μm, $\kappa = 100$, $C_2 = 1$ ppb; curve B, $b - a = 33$ μm, $\kappa = 100$, $C_2 = 1$ ppb; curve C, $b - a = 100$ μm, $\kappa = 10$, $C_2 = 1$ ppb; curve D, $b - a = 100$ μm, $\kappa = 100$, $C_2 = 0.1$ ppb. (b) Mass absorbed by the 1-cm-long fiber in Figure 4 with the same parameters except for the following: curve A, $D_1 = 2.8 \times 10^{-6}$ cm^2/s, $D_2 = 1.08 \times 10^{-4}$ cm^2/s, $d = 0.1$ cm; curve B, $D_1 = 2.8 \times 10^{-6}$ cm^2/s, $D_2 = 1.08 \times 10^{-5}$ cm^2/s, $d = 0.1$ cm; curve C, $D_1 = 2.8 \times 10^{-7}$ cm^2/s, $D_2 = 1.08 \times 10^{-5}$ cm^2/s, $d = 0.1$ cm; curve D, $D_1 = 2.8 \times 10^{-6}$ cm^2/s, $D_2 = 1.08 \times 10^{-5}$ cm^2/s, $d = 0.033$ cm.

than 90% of analyte is in the coating, the distribution coefficient needs to be about an order of magnitude larger then the phase ratio V_2/V_1. In the case discussed in Figure 5a, κ has to be larger than 1000 for quantitative extractions. In a more realistic situation, when using 1 mL of aqueous sample in a vial, the distribution constant needs to be an order of magnitude larger to ensure quantitative extraction.

Figure 5a-A shows the mass absorbed by the fiber over a period of time. This graph was obtained by integrating the area under the curves corresponding to the concentration profiles in the coating illustrated on Figures 4a and b. As discussed previously, the time required for the unstirred solution to reach equilibrium is about 1200 s while the equilibration time for the stirred solution is about 20 s (Figure 3). The rate of mass transport is initially high, but as the water layer around the fiber is depleted, diffusion in water limits the rate of mass transport and slows down the extraction.

Figure 5a, curves A–D, illustrate the effect of changes in experimental parameters on the time extraction profile. A decrease in analyte concentration by an order of magnitude results in an order of magnitude decrease in the mass of analyte extracted by the coating, but the time of extraction is not affected by this change (Figures 5a-A and 5a-D). This is expected since the concentration gradients (and the flux) decreases proportionally with the analyte bulk concentration decrease and therefore equilibration time is not affected. A change in the distribution constant has a significant effect on the time of extraction. By increasing κ by an order of magnitude, the equilibration time increased approximately 4-fold from about 300 s for $\kappa = 10$ (Figure 5a-C) to almost 1200 s for $\kappa = 100$ (Figure 5a-A). This increase is observed because with a larger distribution constant, a larger amount of analyte has to diffuse into the coating before equilibrium is reached. This requires a proportional increase in the analyte flux if the extraction time is to be the same. In the well-agitated case, this was accomplished by an increase in the concentration gradient at the coating/solution interface (Figure 2), and consequently the distribution constant did not affect the equilibration time under this conditions. However, in the static case, transport of analyte is limited by the diffusion in the aqueous layer which reduces the concentration gradient at the the polymer surface and limits the flux. The total amount extracted does not drop by an order of magnitude as would be expected from eq 1 but rather by about a factor of 4 as predicted by eq 24 since the volume of the solution is very small (Figures 5a-A and 5a-C). The 4-fold increase in mass of analyte which needs to be transported into the coating results in a similar increase in the extraction times. A decrease in the coating thickness by a factor of 3 from 100 μm (Figure 5a-A) to about 33 μm (Figure 5a-B) results in a ca. 2-fold decrease in extraction time from almost 1000 s to about 500 s. This decrease is expected since, in this case, the amount of analyte which is required to reach the coating for equilibrium to be established is cut in half.

Figures 4 and 5a suggest that the extraction time in the unagitated case is limited by the transport of analyte in the aqueous phase. Figure 5b provides additional evidence of this. A decrease in the diffusion coefficient of the analyte in water by an order of magnitude from 1.08×10^{-4} cm^2/s (Figure 5b-A) to 1.08×10^{-5} cm^2/s (Figure 5b-B) produced about an order of magnitude increase in equilibration time from about 120 s to about 1200 s. However, a similar change in the diffusion coefficient for the analyte in the polymer coating did not produce a significant change in the corresponding extraction time profiles (Figures 5b-B and 5b-C). In addition, the reduction in vial diameter by a factor of 3 resulted in an order of magnitude decrease in extraction time (Figures 5b-B and 5b-D) from close to 1200 s to about 100 s. These results are consistent with the notion that the transport of analyte through the aqueous phase is the limiting step of the extraction process. In this case, since the average time, t, of the diffusion through the aqueous layer is expected to be proportional to the square of the migration distance, x, and inversely proportional to the diffusion coefficient[5]

$$t = \frac{x^2}{2D_2} \tag{25}$$

This relationship is observed in the above results.

After the extraction is complete, the coated fiber containing the analytes is transferred into the injector of a GC for analysis. This process involves the insertion of the fiber into the injector and the desorption of analytes onto the cryogenically cooled column. During the desorption process, the analyte diffuses from the coating into a stream of carrier gas. Therefore, this process is the reverse of absorption from a well-agitated solution; the only difference being that the aqueous phase is now replaced by a gas. Thus, this situation can be described by the same mathematical model; the initial concentration of analyte in the "solution" is now zero ($C_2^0 = 0$) while the initial concentration of analyte in the coating, C_1^0, is substantial.

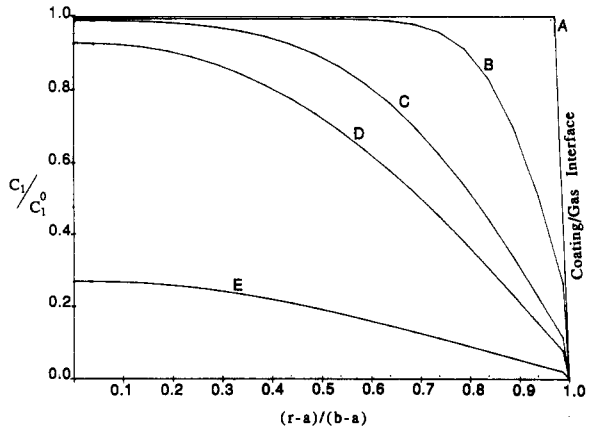

Figure 6. Desorption concentration profile in a fiber coating, with initial analyte concentration carrier gas equal to zero: curve A, $D_1t/(b-a)^2 = 0$; curve B, $D_1t/(b-a)^2 = 0.01$; curve C, $D_1t/(b-a)^2 = 0.05$; curve D, $D_1t/(b-a)^2 = 0.1$; curve E, $D_1t/(b-a)^2 = 0.5$.

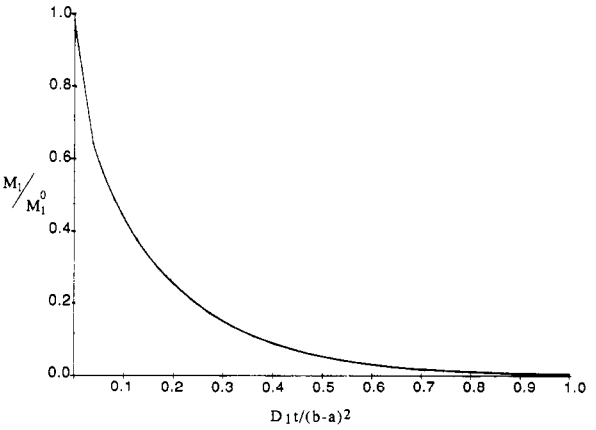

Figure 7. Mass desorbed from a infinite volume stirred fluid with the same parameters as in Figure 4.

This relationship can also be presented graphically. Figure 6 shows a family of curves which describe changes in the concentration profile in the coating during the desorption process. At the start of the desorption, analyte is desorbed from a thin layer of coating near the flowing gas (Figure 6A) and then from deeper inside the coating (Figure 6B–E). The desorption time profile is presented in Figure 7. As in the perfectly agitated case (Figure 3), the desorption process is completed at the time corresponding to $D_1t/(b-a)^2 = 0.5$. The values of the distribution constant and diffusion coefficients are now different because of the different temperatures and the different phases involved. The model predicts that desorption of benzene from the 56-μm-thick coating in an injector held at 140 °C takes place in almost 1 s. This rather fast desorption is due to the fact that the diffusion coefficient of benzene in poly(dimethylsiloxane) increases from 2.8×10^{-6} at 25 °C[6] to 6.7×10^{-5} at 140 °C.[8] It would be rather difficult to verify this prediction using our present experimental setup since it takes a finite amount of time for the fiber to heat up to 140 °C.

EXPERIMENTAL SECTION

Apparatus and Reagents. The SPME device was assembled as in ref 3 with a few modifications. The metal wire plunger assembly of a Hamilton 7105-N syringe (Chromatographic Specialties, Brockville, ON) was replaced with a modified optical fiber (Polymicro Technologies, Tuscon, AZ) which was modified as follows: The total length of fiber used was 6 cm which included 1 cm of poly(dimethylsiloxane)-coated fiber and 5 cm of stripped fiber. The stripping was performed by soaking the section of fiber in concentrated sulfuric acid for 1 min; 1 cm of the uncoated section was inserted into a 15-cm-long metal sheath cut from 1 foot of 30-gauge stainless steel tubing (Chromatographic Specialties, Brockville, ON) and glued in place using epoxy glue. The fiber was then "conditioned" in the injector of a GC by heating it at the maximum injector temperature being used in the GC program for a few minutes. This treatment removed impurities present in the coating introduced during the manufacturing, shipping, and preparation of the fiber.

Fibers with three different coating thicknesses were used. A fiber with a silica o.d. of 111 μm and a total o.d. of 142 μm (the 15-μm-coated fiber), a fiber with a silica o.d. of 112 μm and a total o.d. of 306 μm (the 97-μm-coated fiber), and a fiber with a silica o.d. of 141 μm and a total o.d. of 253 μm (the 56-μm-coated fiber). It should be noted that the manufacturers tolerance on the thicknesses mentioned above is ±13 μm. The coating material of all three fibers was poly(dimethylsiloxane). Nominally 1.8-mL autosampler vials (Chemical Research Supplies, Oakville, ON) were used for all infinite volume experiments (in fact they had a total capacity of about 2.3 mL) while a 1-cm piece cut from a 3-cm-long × 3.3-mm-i.d. autosampler vial insert (Chemical Research Supplies, Oakville, ON) was used for all finite volume experiments.

A Varian 3500 GC equipped with a Septum-equipped programmable injector (SPI) and a flame ionization detector (FID) was used. The glass wool was removed from the 0.8-mm-i.d. insert (Varian, Georgetown, ON) in the SPI prior to use. The GC was also equipped with cryogenics in both the injector and the column. The column used was a 30-m × 0.25-mm DB-1 column (Chromatographic Specialties, Brockville, ON) with 1.0-μm-thick stationary phase. LB-2 septa (Supelco, Oakville, ON) were used in the injector. Septum coring was initially a problem due to the rather thick needle being used. A variety of septa were tested and the LB-2 exhibited the least coring.

A 7-mm × 2-mm spinbar (Bel-Art products, Pequannock, NJ) was used with a magnetic stirrer to stir the solutions while a Branson 2200 sonicator was used in the sonication experiment.

All reagents used were ACS grade (BDH, Toronto, ON). Deionized water was used in all analyses.

Procedure. The 1 μL/mL benzene, toluene, and *p*-xylene standards were prepared in methanol and diluted in water on the day of the analysis since it had been observed that the concentration of benzene in the vials decreased measurably after about 24 h. Vials were filled to the brim with this aqueous solution to prevent the loss of analyte due to the formation of a headspace. For the stirred infinite volume experiments, a spinbar was placed into the vial, 0.05 mL (about 1 drop) of the solution was removed (to prevent the solution wicking up the needle), the septum of the vial was pierced with the syringe needle, and 1 cm of the fiber was exposed to the solution by pushing down on the syringe plunger. After the lapse of a specific time, the plunger was retracted, the needle was removed from the septum of the vial and immediately exposed in the injector of the GC. The time lapse between removal of the fiber from the solution until the start of the GC run was always less than 30 s. Experiments have shown that this time can be as long as 5 min (for the most volatile compound being analyzed, i.e. benzene) with negligible loss of analyte to the atmosphere (submitted to *Environ. Sci. Technol.* University of Waterloo, 1991). A mark was made on the syringe needle such that the fiber would be reproducibly exposed in the injector insert just above the restriction in the insert. The fiber was left inside the injector of the GC for the duration of the analysis. The vial of analyte was discarded after single use so as not to deplete the solution. All experiments were performed in duplicate. The only modification made to the above procedure for the unstirred finite volume experiments was the absence of a stirbar and the use of a 3.2-mm-i.d. vial insert as the analyte container.

The calibration to obtain the actual mass of analyte desorbed from the fiber was done by injecting 0.2 μL of 100 ppm analyte in dichloromethane.

The GC program was as follows: The carrier gas velocity (He) was set at 31 cm/s, the makeup gas flow (N_2) was 25 mL/min, the hydrogen flow was 30 mL/min, and the air flow was 300 mL/min. The injector was started at 25 °C and was immediately ramped at 300 °C/min to 140 °C at which temperature it was held till the end of the run. The column was held at 0 °C for 0.38 min and was then ramped at 50 °C/min to 140 °C at which

temperature it was held for 2.5 min. The detector temperature was held at 300 °C for all runs. The cryogenic focusing involved the cooling of the GC column below room temperature while the injector was rapidly heated, thus trapping the volatiles at the head of the column in a narrow band. After the injector reached its final temperature, the column was heated. The injector was programmed from 25 °C to prevent flashback of the volatile analytes into the needle or even the syringe itself thus adversely affecting the precision and accuracy of the method. The syringe was held in the injector for the duration of the run.

Computer programs were written using Asyst (Asyst Software Technologies Inc., Rochester, NY) to calculate both of the mathematical models developed during this work.

DISCUSSION OF EXPERIMENTAL RESULTS

The liquid polymer used as a fiber coating material in all of our investigations was poly(dimethylsiloxane). There are several important reasons why this material was chosen. Optical fibers coated with this polymer are commercially available in a variety of thicknesses. The polymer is a commonly used nonpolar and thermally stable (up to about 300 °C) GC stationary phase. The glass transition temperature of this polymer is −126 °C,[9] and its melting point is −50 °C;[10] both temperatures are significantly below the temperatures encountered in either the extraction or the desorption processes. Thus no complications due to phase transitions are expected with this material. In addition, since the coating is a viscous liquid polymer which is above its glass transition temperature, the diffusion coefficients of the analyte in it will be orders of magnitude lower than its diffusion coefficient in a solid polymer which is below its glass transition temperature. Therefore, since the dynamics of mass transport in a well-stirred solution is controlled by the diffusion coefficient of the analyte in the coating, the extraction time required with a liquid polymer coating will be considerably less than that required with a solid polymer. Benzene and its substituted derivatives were used as test analytes because they are common contaminants of water supplies, because they are expected to have a reasonably high distribution constant between water and the polymer, and because of the substantial amount of physicochemical data available on these compounds.

From the theory it is clear that for rapid extractions, an efficient means of agitating the solution is required. Under these conditions the static aqueous layer which forms in solution close to the surface of the fiber is very thin. If "perfect mixing" is achieved, mass transport is only limited by the diffusion of analyte in the coating. To investigate the best means of agitation, a variety of methods were tested (Figures 8 and 9). Figure 8 represents the results obtained by the more traditional means of agitation, i.e. stirring. The test analyte is 1 ppm benzene in deionized water and the extraction was done using the 56-μm-thick poly(dimethylsiloxane) coating. The "percent" values correspond to positions on the dial of the stirrer. Curves A–E (Figure 8) clearly show that the extraction time profiles are dramatically affected by the stirring rate. The 100% stirred case takes approximately 100 s to reach equilibrium (Figure 8B) while theory predicts 20 s (assuming perfect agitation conditions, see Figure 8A). The theoretical value is calculated by using 2.8×10^{-6} cm^2/s[6] as the diffusion coefficient of benzene in poly(dimethylsiloxane). It should be noted that since the length of the polymer chains, their shape, and the degree of cross-linking in polymers varies with the method of synthesis used, some variation between diffusion properties of polymers are expected. However, since the experimental equilibration time is several times longer than the theoretical value, it indicates that under these conditions, the solution is not agitated efficiently enough to ensure that the absorption process is limited only by mass transport through the polymer. Figure 8 illustrates that as a consequence of decreasing stirring rates, mass transport through

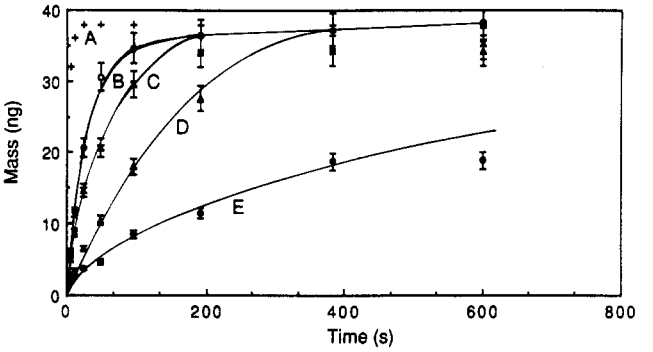

Figure 8. Effect of stirring on the absorption profile of 1 ppm benzene in water extracted with a 56-μm-thick coating on a 1-cm-long fiber. (A) + = theory, (B) ○ = 100% stirred, (C) × = 75% stirred, (D) △ = 50% stirred, (E) ● = unstirred.

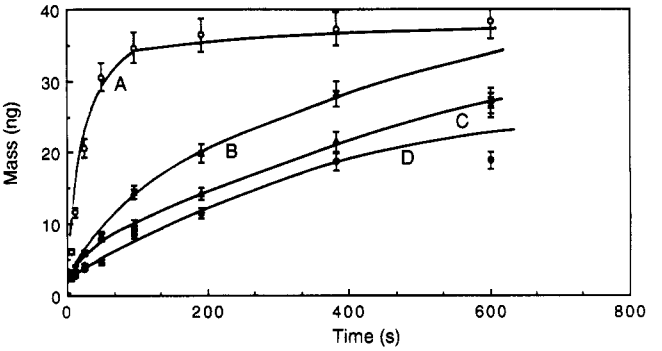

Figure 9. Effect of agitation method on the absorption profile of 1 ppm benzene in water extracted with a 56-μm coating on a 1-cm-long fiber. (A) ○ = 100% stirred, (B) × = sonicated, (C) △ = fiber insertion/retraction, (D) ● = unstirred.

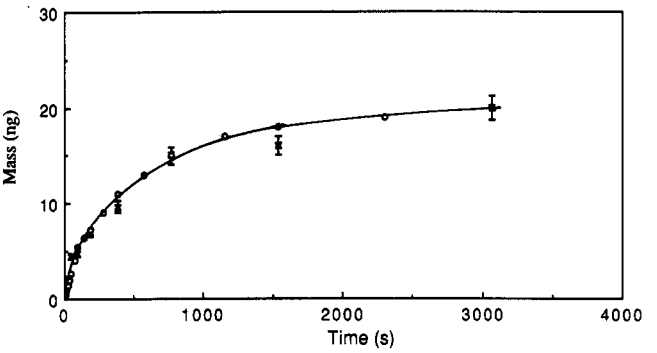

Figure 10. Absorption profile of an unstirred, finite volume (about 100 μL) solution of 1 ppm benzene in water extracted with a 56-μm-thick coating on a 1-cm-long fiber, × = experiment, ○ = theory.

the progressively thicker stationary aqueous layer results in increased extraction times (Figures 8B–D). The equilibration time is about 150 s for the 75% stirred rate (Figure 8C) and almost 300 s for the 50% stirred rate (Figure 8D). When the solution is not stirred, Figure 8E, the extraction process is only 50% completed after about 600 s. In fact, the time required to reach equilibrium in a static solution is about 1200 s, as in Figure 10 which illustrates the relationship for longer exposure time range. In Figure 10 both the theoretical and experimental exposure profile data for the same geometric configuration is plotted. The experimental relationship matches the theoretical predictions. The value for the distribution constant determined independently from Figure 8 was used in the calculations. Here, too, the literature diffusion coefficient of 2.8×10^{-6} cm^2/s[6] was used. In this experiment a small volume and narrow (about 1.6-mm i.d.) container was used. Therefore the effects of fluid convection was greatly reduced. When using larger volume vials, this mechanism of

mass transport should be considered when modelling the extraction process in static solution.

We also considered less conventional means of agitating the solution. Figure 9 illustrate these results. Sonication (using a laboratory glassware cleaner) improves mass transport compared with the unstirred case but is still not as efficient as stirring at the maximum rate (Figures 9A and 9B). The time absorption profile curve corresponding to sonication are similar to the 50% stirred case (Figure 8D). This result is quite encouraging considering the poor efficiency of sonic energy transfer through the thick-walled glass vials. Sonication using higher power coupling horns should improve mixing substantially. The last means of agitation investigated involved the insertion and retraction of the fiber into and out of the solution at the rate of one insertion/retraction per second (Figure 9C). Here we attempted to minimize the thickness of the static layer at the surface of the fiber by moving the fiber as opposed to the water. The reduction in extraction time is small compared with the unstirred case as shown on Figure 9D. However the effect is more substantial than may be apparent from examining Figure 9 since in this experiment, the fiber spent only half of the extraction time in the bulk of the aqueous solution. The agitation efficiency should improve substantially when combining this method with sonication or mixing. The whole process of mixing can be automated by using an autosampler which can be programmed to move the fiber. Considering the above results, 100% stirring was used in all further investigations since it proved to be the most effective and widely available method.

As can be seen from Figures 8 and 9, the 56-μm-thick coating absorbed about 38 ng of benzene from 2.3 mL of 1 ppm benzene in water. This is about 2% of the total amount of analyte initially in the vial. When a smaller volume was used (about 0.1 mL), the mass of analyte extracted at equilibrium was only half that of the previous case and the extraction exhausts about 25% of the total amount of analyte initially in the vial (Figure 10). In the latter case, multiple extractions from the same vial can exhaust the solution very quickly, and thus multiple extractions with on-column cryofocusing can be used to achieve quantitative extractions.

One way to improve the sensitivity of the method is to use a thicker coating thus increasing the coating:solution volume ratio. By doubling the volume of the coating, the mass of analyte absorbed at equilibrium doubles. This can be confirmed by comparing the mass absorbed by the 56-μm-thick coating (about 40 ng, Figure 11B) with the mass absorbed by the 97-μm-thick coating (about 80 ng, Figure 11A). But a thicker coating also increases the equilibration time from approximately 100 s to about 200 s. The model which considers diffusion through water as a limiting step (i.e. the unagitated model) predicts that if the mass of compounds absorbed doubles, the equilibration time also doubles. On the other hand, the model which considers diffusion through the coating as the limiting step (i.e. the agitated model) predicts that if the coating thickness doubles, the equilibration time quadruples. Experimentally, there is a doubling of the equilibration time which confirms the assumption made before about the transport limit set by diffusion of analyte in water. The mass absorbed is reduced to below 10 ng and the equilibration time to about 30 s when thin, 15 μm, coating was used.

The relative error in our results obtained for benzene is inversely related to the thickness of coating used. For example, for the 97-μm-thick coating the error is 0.63%, for the 56-μm coating it is 6.3%, and for the 15-μm coating it is 12%. This is caused by the fact that analyte loss to the atmosphere during the transport of the fiber from the extraction vial to the injector of the GC is dependent on the surface area to volume ratio of the coating. This ratio increases as the thickness of the coating decreases. A random error caused by the variation in the time spent between extraction and injection is thus introduced.

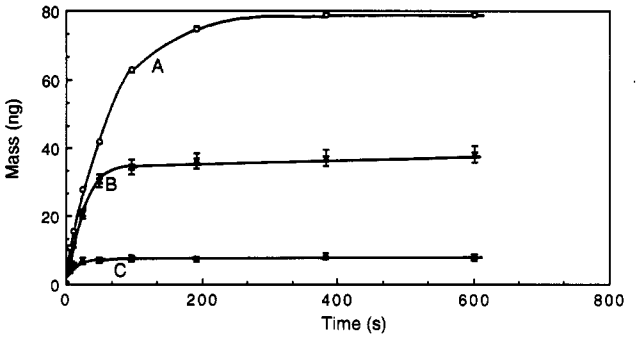

Figure 11. Effect of coating thickness on the absorption profile of 100% stirred 1 ppm benzene extracted with a 1-cm-long fiber. (A) O = 97 μm, (B) × = 56 μm, (C) Δ = 15 μm.

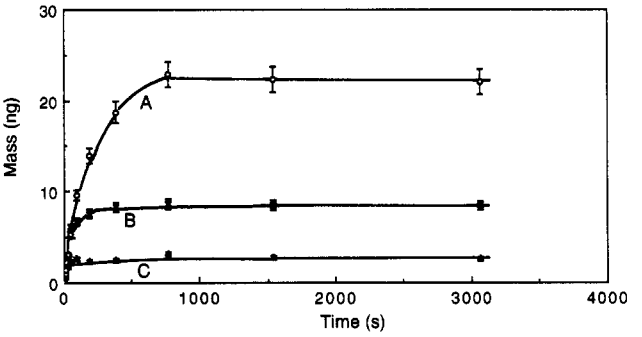

Figure 12. Effect of distribution constant on the absorption profile of 100% stirred 0.1 ppm analyte extracted with a 56-μm-thick coating on a 1-cm-long fiber. (A) O = *p*-xylene, (B) × = toluene, (C) Δ = benzene.

The thickness of the coating determines the volume of the stationary phase and consequently the sensitivity of the method. To increase the mass absorbed a longer piece of fiber can be exposed to aqueous sample. However if the length exceeds 2 cm, a larger vial would be needed while if it is any longer than about 4 cm, modifications will have to be made to the GC injector setup.

The other parameter which controls the mass of analyte absorbed by the fiber is the coating/water distribution constant of the analyte. Figure 12 shows the extraction profiles of 0.1 ppm benzene, toluene, and *p*-xylene in water. Based on these results, the poly(dimethylsiloxane)/water distribution constant of each analyte was determined. The distribution constant of benzene is 125 (Figure 12C), that of toluene is 294 (Figure 12B), and that of *p*-xylene is 831 (Figure 12A). They are calculated by using the mass of analyte extracted by the coating at equilibrium and using eq 25. These values are in most of the cases close to the literature data for the octanol/water distribution constants of these analytes, which are 135 for benzene, 447 for toluene, and 1510 for *p*-xylene.[11] This correlation is expected since the magnitude of this constant is related to the polarity of the compounds. Thus, the selectivity of the poly(dimethylsiloxane) coating is also related to the polarity of the analyte. It should be recognized that the accuracy of the distribution constant data measured in this simple experiment using the commercial coating is very poor because of large diameter tolerances given by the manufacturers (see the Experimental Section). This situation can be significantly improved by using geometrically well-defined fibers.

The selectivity of the coating for the analyte can be improved by modifying the chemical structure of the polymer as is commonly done in gas chromatography. Thus, if polar

liquids are coated onto the fiber, more polar compounds can be analyzed at low concentrations.

Figure 12 also shows the dramatic difference in equilibration time for the three analytes. The equilibrium time increases from about 100 s for benzene to about 200 s for toluene and to almost 600 s for *p*-xylene. If we assume a perfectly agitated solution, this result would be unexpected since in this model the extraction time is only dependent on the diffusion coefficient of the analyte in the coating of given thickness. It seem unlikely that the diffusion coefficients of the three analytes vary so widely. However, this result is expected from the finite volume, unstirred solution model. In the latter model, the higher distribution constant of toluene and *p*-xylene relative to benzene requires that a larger amount of analyte be transported to the surface of the fiber. The flux of analytes into the coating is approximately constant for benzene, toluene, and xylene since it is determined by the diffusion though the aqueous layer adjacent to the fiber and since their diffusion coefficients are similar because the molecules have similar size.[8] The difference in equilibration time is evident when analyzing the effect of stirring rate on the extent of extraction of the three analytes after a 10-min exposure (Table I). Benzene has reached equilibrium already for the 50% stirring rate while *p*-xylene has not equilibrated even at the 75% stirring rate. The amount of xylene extracted at the 75% rate is significantly below the value for the 100% stirring rate.

Equations 1 and 25 indicates that there is a linear relationship between the concentration of analyte in solution and the mass of analyte in the coating at equilibrium. Figure 13 illustrates the extraction profiles for three concentrations of benzene in water. As expected, the mass of analyte extracted is linearly proportional to the concentration of analyte in solution while the extraction time is unaffected. This result is expected when considering both the static and the well agitated models. This independence of extraction time from concentration of analyte simplifies the use of SPME since it is not necessary to obtain time exposure profiles for a range of concentrations in order to do quantitative analysis.

The 0.1 ppm solution analyzed with the 56-μm-thick coating produces a signal-to-noise ratio of about 500:1 when using a flame ionization detector (FID). This result is expected considering that about 3 ng of sample were extracted from the solution (Figure 13C) and the detection limit of an FID is about 1 pg/s. This would indicate that the limit of quantitation of this technique is approximately 0.6 ppb with a 56-μm-thick coating for this detector. Lower detection limits are expected when thicker or if more selective coatings or more sensitive detectors are used. For example, in the above case ppt sensitivities are expected when applying a photoionization detector. Even a conventional quadrupole mass spectrometer in the selective ion monitoring mode or an ion trap mass spectrometer in the full scan mode is expected to quantitate ppt levels of benzene. The larger less polar molecules with higher octanol/water distribution constants are expected to have proportionally lower limits of detection when using a piece of poly(dimethylsiloxane)-coated fiber.

CONCLUSIONS

Compared to commonly used isolation techniques, the advantages of SPME include the complete elimination of organic solvents, the simplification of analytical extractions, improvement in precision, and savings of time and money.[12-16] SPME can be used to determine traces of organic contaminants at sub-ppb levels which makes it an ideal method for the analysis of drinking and waste waters. Although, in most cases, it is expected that only a small portion of analyte is absorbed from the aqueous sample into the coating, the procedure facilitates high sensitivity analysis since the total amount of extracted material is transferred onto the column.

Table I. Effect of Stirring on Equilibration Time of Three Analytes

analyte	100% stirred (×10³ area counts)	75% stirred (×10³ area counts)	50% stirred (×10³ area counts)	0% stirred (×10³ area counts)
benzene	237	234	251	120
toluene	739	730	688	349
p-xylene	1873	1791	1175	407

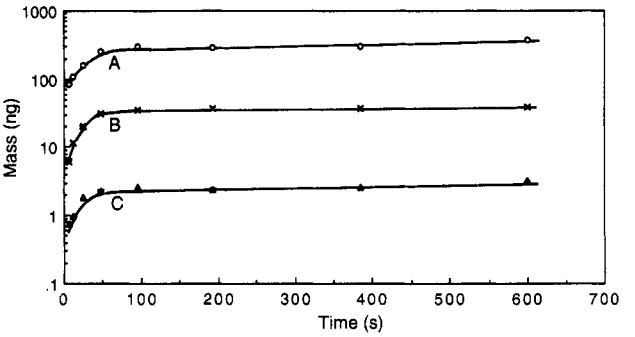

Figure 13. Effect of analyte concentration on the absorption profile of 100% stirred benzene in water extracted with a 56-μm-thick coating on a 1-cm-long fiber. (A) O = 10 ppm, (B) × = 1 ppm, (C) Δ = 0.1 ppm.

The detection limit of the method for a given analyte is dependent on the selectivity (i.e. the coating/water distribution constant) and the thickness of the coating (i.e. the volume of organic phase) used. These parameters determine what fraction of the analyte initially present in solution is extracted by the coating. General purpose nonpolar coatings such as the poly(dimethylsiloxane) polymer discussed in this paper can be used effectively in wide-range screening applications. The selectivity of this material can be approximated by the use of octanol/water distribution constants. Sub-ppb detection limits are attainable for molecules such as benzene, toluene, and *p*-xylene; more environmentally interesting lipophilic compounds will have higher distribution constants, and consequently lower detection limits are expected for these analytes. Polar organic coatings can be designed which could more effectively extract more hydrophilic compounds such as phenols and most pesticides which are difficult to analyze by the commonly used methods.

To use SPME in quantitative analysis, one needs to determine the coating/water distribution constant of the analyte. Therefore, calibration curves are required for each of the analytes. The distribution constant determines the slope of the calibration curve for a given coating thickness. The situation is similar to liquid chromatographic separations where the retention time of solute is proportional to the stationary/mobile phase distribution constant. The partition coefficient is affected by temperature variations and the composition of the aqueous matrix caused by the presence of salts (changes in ionic strength) or high levels of organic interferences (changes in polarity index). However, as in liquid chromatography, these effects are not expected to be very large for below 1% concentration levels of components and small temperature changes which are usually associated with the laboratory environment. The preliminary results reported previously support this postulate.[3] These conditions are met in the majority of analytical situations. For other cases the changes can be accounted for by using C-13-labeled internal standards or by using the standard additions quantitation method. In addition experimental conditions can be altered to achieve quantitative extraction for example by using thicker, more selective coatings or by using salting-out techniques.

The extraction time in practical cases is controlled by the efficiency of the mixing technique used. Agitation efficiency is particularly important for analytes with high coating/water distribution constants. If the agitation is perfect and the thin layer of unstirred water around the fiber is very small and can be ignored, even high molecular weight compounds can be analyzed in a very short time (under 100 s). Analytes with high coating/water distribution constants do not require the use of thick coatings to achieve good sensitivities. A thin coating can be used which will reduce the extraction time even further.

The mass-transfer limitation caused by the diffusion of analyte in the aqueous phase may be overcome by sampling volatile analytes from the headspace above the aqueous sample since diffusion coefficients of molecules in the gas phase are about 4 orders of magnitude higher than in water. This approach will also eliminate the matrix effects discussed above. The efficiency of this indirect extraction can be improved by ensuring rapid mass transfer between the aqueous and vapor phases. The use of a spray system may help in this regard.

The utility of SPME is not limited to aqueous samples. Other fluids such as organic solvents, gases, supercritical fluids and even volatile contaminants in solids can be analyzed by using this method combined with the headspace technique. Nor is SPME limited to the analysis of organic contaminants with a gas chromatograph; it can be used, with minor modifications, in isolating and transferring analytes from a matrix to a mass spectrometer. By modifying the silica surface with the appropriate material, SPME can be used to extract ionic species from a sample and then be used as a direct insertion probe in an inductively coupled plasma atomic emission spectrophotometer. SPME is not limited to environmental applications; in clinical analysis, target compounds can be extracted in vivo from bodily fluids without removing them from the living organism. In industrial process control analysis target, analytes in corrosive or toxic fluids can be conveniently sampled.

SPME can also be used to provide useful physicochemical data on various compounds and coating materials. As discussed earlier, distribution constants can be easily determined from the amount of analyte extracted at equilibrium. Activity coefficients of various analytes in different liquids can be measured. If the analyte solution is sufficiently agitated, especially in the gas phase, the shape of the time extraction profile allows the determination of diffusion coefficients in coatings. Diffusion coefficients of various compounds in different liquids can also be determined when using static extraction conditions. Chemical and thermal degradation of the coating material can be investigated by using selective probe molecules.

The discussion in this paper was limited to the polymers which are normal liquids at room temperature. The analogous investigations, although much more theoretically complex, can be performed for materials which are below their glass transition and melting points when considering activation energy of absorption at the interface and swelling effects.[17] These processes are expected to substantially increase the extraction times. The above results are not only critical in understanding the dynamics of extraction using fibers but they are also helpful in considering more complex particle geometries associated with the traditional solid-phase extraction method.

ACKNOWLEDGMENT

We wish to thank Catherine L. Arthur for her invaluable discussions and help with the experimental setup. The assistance of Dr. Mark Pritzker in deriving the mathematical models is greatly appreciated. This work was supported in part by the Natural Sciences and Engineering Research Council of Canada, Varian Canada Inc., and Imperial Oil of Canada.

GLOSSARY

n_1	number of moles of analyte in coating
n_2	number of moles of analyte in solution
V_1	volume of coating
V_2	volume of solution
C_1	concentration of analyte in coating
C_2	concentration of analyte in solution
C_1^0	initial concentration of analyte in coating ($t = 0$)
C_2^0	initial concentration of analyte in solution ($t = 0$)
C_1^∞	concentration of analyte in coating at equilibrium ($t = \infty$)
C_2^∞	concentration of analyte in solution at equilibrium ($t = \infty$)
M_1	mass of analyte in coating
M_2	mass of analyte in solution
M_1^0	initial mass of analyte in coating ($t = 0$)
M_2^0	initial mass of analyte in solution ($t = 0$)
M_1^∞	mass of analyte in coating at equilibrium ($t = \infty$)
M_2^∞	mass of analyte in solution at equilibrium ($t = \infty$)
L	length of coated fiber
a	radius of fused silica rod
b	radius of coated fiber
d	radius of vial
D_1	diffusion coefficient of analyte in coating
D_2	diffusion coefficient of analyte in solution
κ	coating/water distribution constant of analyte
r	distance from the center of the fiber rod

APPENDIX

Derivation of the Stirred Infinite-Volume Model. Equations 4, 6, 7, and 8 were transformed by the substitution

$$\phi(r,t) = C_1(r,t) - \kappa C_2^0 \tag{26}$$

Using the technique of separation of variables,[18] we assumed that $\phi(r,t)$ can be separated into time and radius dependent components:

$$\phi(r,t) = \Psi(r)\Gamma(t) \tag{27}$$

We then substitute eq 27 into eq 4 and write the result such that one side of the equation is only a function of time and the other only a function of radius:

$$\frac{1}{\Gamma}\frac{d\Gamma}{dt} = \frac{D_1}{\Psi}\frac{d^2\Psi}{dr^2} + \frac{D_1}{\Psi r}\frac{d\Psi}{dr} \tag{28}$$

To ensure that this equation is valid for any given time and radius, each side must be a constant (called the separation constant, λ). Thus we reduced a partial differential equation to an ordinary differential equation. First, we consider the time-dependent part:

$$\frac{d\Gamma}{dt} - \lambda\Gamma = 0 \tag{29}$$

which has the solution:

$$\Gamma = Ce^{\lambda t} \tag{30}$$

Next, we consider the time-independent part:

$$\frac{D_1}{\Psi}\frac{d^2\Psi}{dr^2} + \frac{D_1}{\Psi r}\frac{d\Psi}{dr} = \lambda \tag{31}$$

We rearrange all the terms to one side of the equation and make the substitution:

$$\alpha^2 = -\frac{\lambda}{D_1} \tag{32}$$

into eq 31. The resulting equation is an example of a Sturm–Liouville differential equation:[19]

$$\frac{d^2\Psi}{dr^2} + \frac{1}{r}\frac{d\Psi}{dr} + \alpha^2\Psi = 0 \tag{33}$$

we multiply eq 33 by r^2 and make the substitution $x = \alpha r$ and obtain Bessel's equation of order zero:[19]

$$x^2\frac{d^2\Psi}{dx^2} + x\frac{d\Psi}{dx} + x^2\Psi = 0 \tag{34}$$

This is solved by the method of Frobenius[18] with the solution

$$\Psi = AJ_0(x) + BY_0(x) \tag{35}$$

where $J_0(x)$ and $Y_0(x)$ are Bessel functions of the first and second kind, respectively. We then transform back to r space and now we have the general solution to our differential equation:

$$\phi(r,t) = e^{-\alpha^2 D_1 t}[AJ_0(\alpha r) + BY_0(\alpha r)] \tag{36}$$

We now apply the boundary conditions to determine the constants in the general solution by using the useful equations

$$\frac{d}{dr}J_0(\alpha r) = -\alpha J_1(\alpha r) \tag{37}$$

and

$$\frac{d}{dr}Y_0(\alpha r) = -\alpha Y_1(\alpha r) \tag{38}$$

and by forcing

$$J_1(\alpha a)Y_0(\alpha b) - J_0(\alpha b)Y_1(\alpha a) = 0 \tag{39}$$

so that we obtain a nontrivial solution. We now have a solution:

$$\phi(r,t) = e^{-\alpha^2 D_1 t}\frac{A}{Y_0(\alpha b)}[Y_0(\alpha b)J_0(\alpha r) - J_0(\alpha b)Y_0(\alpha r)] \tag{40}$$

To simplify the equations, we define

$$R_0(\alpha r) = Y_0(\alpha b)J_0(\alpha r) - J_0(\alpha b)Y_0(\alpha r) \tag{41}$$

and allow the constant A to absorb the constant $Y_0(\alpha b)$. The resulting equation satisfies the boundary conditions. We now need to satisfy the initial condition. Note that eq 4 is linear and that the boundary conditions are homogeneous. We represent eq 4 using the differential operator L:

$$L = \frac{\partial}{\partial t} - D_1\left(\frac{\partial^2}{\partial r^2} + \frac{1}{r}\frac{\partial}{\partial r}\right) = 0 \tag{42}$$

Thus L is a linear operator and thus if there were two solutions, ϕ_1 and ϕ_2, $\phi_1 + \phi_2$ would also be a solution:

$$L(\phi_1 + \phi_2) = L(\phi_1) + L(\phi_2) \tag{43}$$

So we can find a number of solutions to eq 4 and their sum will also satisfy our boundary conditions. It turns out that eq 40 has infinitely many roots, α_n and we write

$$C_1^0 - \kappa C_2^0 = \sum_{n=1}^{\infty} A_n R_0(\alpha_n r) \tag{44}$$

We multiply both sides by $rR_0(\alpha_m r)$ and integrate from a to b, the interior and exterior surface radii. But, $R_0(\alpha_n r)$ is a solution to a Sturm–Liouville differential equation with the weight factor of r. Thus, all terms on the left hand side of eq 44 vanish except for the term where $n = m$. We evaluate the integral

$$(C_1^0 - \kappa C_2^0)\int_a^b rR_0(\alpha_m r)dr = A_m N(\alpha_m r) \tag{45}$$

and obtain

$$\frac{1}{N(\alpha_m r)} = \frac{\pi^2\alpha_m^2 J_1^2(\alpha_m a)}{2[J_1^2(\alpha_m a) - J_0^2(\alpha_m b)]} \tag{46}$$

We also need to evaluate the integral

$$\int_a^b rR_0(\alpha_m r)\,dr = \int_a^b r[J_0(\alpha_m r)Y_0(\alpha_m r) - J_0(\alpha_m b)Y_0(\alpha_m r)]\,dr \tag{47}$$

Using the relationship

$$\int rJ_0(\alpha r)\,dr = \frac{rJ_1(\alpha r)}{\alpha} \tag{48}$$

and

$$\int rY_0(\alpha r)\,dr = \frac{rY_1(\alpha r)}{\alpha} \tag{49}$$

and using the Wronskian relationship for Bessel functions,[18] eq 47 simplifies to $2/\pi\alpha^2$. We substitute this result and eq 46 into eq 45 and rearrange and backtransform the result using eqs 40 and 26, respectively, and obtain the final result, eq 9.

Derivation of the Unstirred Solution Model. We break up our region into intervals of width Δr so that

$$r = i\Delta r \tag{50}$$

Thus, $i = 0$ at the silica/coating interface, $i = M$ at the coating/solution interface and $i = N$ at the solution/vial interface. And we also break up our time into intervals of period Δt so that

$$t = n\Delta t \tag{51}$$

We approximate the radius first derivatives in two different ways, using central difference[20]

$$\frac{\partial C_j}{\partial r} = \frac{C_{j\,i+1}^{\,n} - C_{j\,i-1}^{\,n}}{2\Delta r} \tag{52}$$

(where n denotes the nth time mesh line and i denotes the ith radius mesh line) and backward difference[20]

$$\frac{\partial C_j}{\partial r} = \frac{C_{j\,i}^{\,n} - C_{j\,i-1}^{\,n}}{\Delta r} \tag{53}$$

We will approximate the second derivative using central difference

$$\frac{\partial^2 C_j}{\partial r^2} = \frac{C_{j\,i-1}^{\,n} - 2C_{j\,i}^{\,n} + C_{j\,i+1}^{\,n}}{(\Delta r)^2} \tag{54}$$

and the time derivative as follows:

$$\frac{\partial C_j}{\partial t} = \frac{C_{j\,i}^{\,n} - C_{j\,i}^{\,n-1}}{\Delta t} \tag{55}$$

Now we substitute eqs 50, 52, 53, and 54 into eq 4:

$$\frac{C_{j\,i-1}^{\,n} - 2C_{j\,i}^{\,n} + C_{j\,i+1}^{\,n}}{(\Delta r)^2} + \frac{1}{i\Delta r}\left[\frac{C_{j\,i+1}^{\,n} - C_{j\,i-1}^{\,n}}{2\Delta r}\right] = \frac{1}{D_j}\left[\frac{C_{j\,i}^{\,n} - C_{j\,i}^{\,n-1}}{\Delta t}\right] \tag{56}$$

Equation 52 is substituted into eq 8, and the result is substituted into eq 56 evaluated at $r = a$ to give

$$\frac{2(C_{1\,i+1}^{\,n} - C_{1\,i}^{\,n})}{(\Delta r)^2} = \frac{1}{D_1}\left[\frac{C_{1\,i}^{\,n} - C_{1\,i}^{\,n-1}}{\Delta t}\right] \tag{57}$$

which is valid for all points that lie on the interior boundary $r = a$. We substitute eq 52 into eq 15, and the result is substituted into eq 56 evaluated at $r = d$ to obtain

$$\frac{2(C_{2\,i-1}^{\,n} - C_{2\,i}^{\,n})}{(\Delta r)^2} = \frac{1}{D_2}\left[\frac{C_{2\,i}^{\,n} - C_{2\,i}^{\,n-1}}{\Delta t}\right] \quad (58)$$

which is valid for all points that lie on the exterior boundary $r = d$. We then substituted eq 54 into eq 14 to obtain

$$D_1\left[\frac{C_{1\,i}^{\,n} - C_{1\,i-1}^{\,n}}{\Delta r}\right] = D_2\left[\frac{C_{2\,i+1}^{\,n} - C_{2\,i}^{\,n}}{\Delta r}\right] \quad (59)$$

which is valid for all points that lie at the interface between the two regions, i.e. at $r = b$. Boundary condition eq 7 is simply

$$C_{1\,i}^{\,n} = \kappa C_{2\,i}^{\,n} \quad (60)$$

and is also valid for all points that lie at $r = b$. The initial conditions are thus

$$C_{1\,i}^{\,0} = C_1^{\,0} \quad (61)$$

and

$$C_{2\,i}^{\,0} = C_2^{\,0} \quad (62)$$

Now we determine the concentrations at intervals of Δr along the radius. We thus need to determine the concentrations $C_{1\,1}, C_{1\,2}, C_{1\,3}, ..., C_{1\,M-1}, C_{1\,M}, C_{2\,M}, C_{2\,M+1}, ..., C_{2\,N}$. Thus there are $N + 1$ concentrations to determine using $N + 1$ equations (1 from eq 57, $M - 2$ from eq 56, 1 from eq 59, 1 from eq 60, $N - M - 1$ from eq 56, and 1 from eq 58). For each value of n (i.e. at each time), we have to solve a system of $N + 1$ simultaneous linear equations. At each time we know that C^{n-1}'s and we want to solve for the C^n's. Rearranging eq 57 we obtain eq 16, rearranging eq 56 we obtain eq 17, rearranging eq 59 we obtain eq 18, rearranging eq 60 we obtain eq 19, rearranging eq 56 we obtain eq 20, and rearranging eq 58 we obtain eq 21.

Registry No. C_6H_6, 71-43-2; $C_6H_5CH_3$, 108-88-3; $H_3CC_6H_4$-p-CH_3, 106-42-3; H_2O, 7732-18-5; fused silica, 60676-86-0.

REFERENCES

(1) Suffet, I. H., Malaiyandi, M., Eds. *Advances in Chemistry, Series, Vol. 214: Organic Pollutants in Water: Sampling, Analysis, and Toxicity Testing*; American Chemical Society: Washington, D.C., 1987.
(2) Clesceri, L. S., Greenberg, A. E., Trussell, R. R., Eds.; *Standard Methods for the Examination of Water and Wastewater*, 17th ed.; American Public Health Association: Washington, D.C., 1989.
(3) Arthur, C. L.; Pawliszyn, J. *Anal. Chem.* **1990**, *62*, 2145–2148.
(4) Belardi, R. G.; Pawliszyn, J. *Water Pollut. Res. J. Can.* **1989**, *24*, 179.
(5) Crank, J. *The Mathematics of Diffusion*, 2nd ed.; Clarendon Press: Oxford, U.K., 1989.
(6) Newns, A. C.; Park, G. S. *J. Polym. Sci.: Part C* **1969**, *22*, 927–937.
(7) Wendt, J. O. L.; Frazier, G. C., Jr. *Ind. Eng. Chem., Fundam.* **1973**, *12* (2), 239–243.
(8) Van Krevelen, D. W. *Properties of Polymers: Their Estimation and Correlation with Chemical Structure*, 2nd ed.; Elsevier Scientific Publishing Company: Amsterdam, The Netherlands, 1976.
(9) Brandrup, J.; Immergut, E. H. *Polymer Handbook*, 3rd ed.; John Wiley and Sons Inc.: New York, 1989.
(10) Ohlberg, S. M.; Alexander, L. E.; Warrick, E. L. *J. Polym. Sci.* **1958**, *27*, 1.
(11) Miller, M. Michele et al. *Environ. Sci. Technol.* **1985**, *19* (6), 522–529.
(12) Keith, L. H. *Advances in the Identification and Analysis of Organic Pollutants in Water, Vol. 2*; Butterworths: Sevenoaks, U.K., 1981.
(13) Van Hall, C. E.; Editor *ASTM Special Technical Publication 686: Measurement of Organic Pollutants in Water and Wastewater*. [Proceedings of a Symposium Held in Denver, 19–20 June 1978]; ASTM: Philadelphia, PA, 1979.
(14) Keith, Lawrence H. *Advances in the Identification and Analysis of Organic Pollutants in Water, Vol. 1*; Butterworths: Sevenoaks, U.K., 1981.
(15) Liska, I.; Krupcik, J.; Leclercq, P. A. *J. High Resolut. Chromatogr.* **1989**, *12* (9), 577–90.
(16) Leithe, W. *Analysis of Organic Pollutants in Water and Waste Water* Ann Arbor Science Publ.: Ann Arbor, MI, 1973.
(17) McGregor, R. *Diffusion and Sorption in Fibers and Films*; Academic Press: London, U.K., 1974.
(18) Boyce, W. E.; DiPrima, R. C. *Elementary Differential Equations and Boundary Value Problems*, 4th ed.; John Wiley and Sons, Inc.: New York, 1986.
(19) Spiegel, M. R. *Applied Differential Equations*, 3rd ed.; Prentice-Hall, Inc.: Englewood Cliffs, NJ, 1981.
(20) Riggs, J. B. *An Introduction to Numerical Methods for Chemical Engineers*; Texas Tech University Press: Lubbock, TX, 1988.

RECEIVED for review October 1, 1991. Accepted January 21, 1992.

CORRESPONDENCE

Exchange of Comments on Convergence of Generalized Simulated Annealing with Variable Step Size with Application toward Parameter Estimations of Linear and Nonlinear Models

Sir: In a recent article in this journal, Sutter and Kalivas have suggested that the technique of generalized simulated annealing (GSA) can be modified for good use in fitting data to functions.[1] The GSA technique was developed to find global minima or maxima associated with response surfaces. These authors show that the addition of a variable step size (designated as VSGSA) to GSA results in improved fitting of two examples previously treated with a simplex optimization by Zupan and Rius.[2] The present communication is not concerned with response surface methodology. We specifically address the issue of whether VSGSA converges to optimum parameter values in the two examples of data fitting given by Sutter and Kalivas.

It is somewhat surprising that neither pair of authors compared the results of their fitting techniques with the well-established procedure of using nonlinear least squares to fit data to a given function. Nonlinear least squares has a substantial history of being extremely useful for this purpose and is almost certainly the most generally applicable technique. A number of examples and pertinent references are given in the review article by Rusling.[3]

We have refit the data used by Sutter and Kalivas by two related processes. The first process uses a general purpose nonlinear least squares approach (using a Marquardt–Levenberg algorithm), and the second uses an approach which considers the problem as a set of simultaneous equations to be solved.[4,5] The best-fit criterion for our treatment is the same as that used in refs 1 and 2 (designated by OC there);

0003-2700/92/0364-1199$03.00/0